

Phenotypic characterization of *Bbs4* null mice reveals age-dependent penetrance and variable expressivity

Erica R. Eichers · Muhammad M. Abd-El-Barr · Richard Paylor ·
Richard Alan Lewis · Weimin Bi · Xiaodi Lin · Thomas P. Meehan ·
David W. Stockton · Samuel M. Wu · Elizabeth Lindsay · Monica J. Justice ·
Philip L. Beales · Nicholas Katsanis · James R. Lupski

Received: 22 February 2006 / Accepted: 28 April 2006 / Published online: 23 June 2006
© Springer-Verlag 2006

Abstract Bardet-Biedl syndrome (BBS) is a rare oligogenic disorder exhibiting both clinical and genetic heterogeneity. Although the BBS phenotype is variable both between and within families, the syndrome is characterized by the hallmarks of developmental and learning difficulties, post-axial polydactyilia, obesity, hypogenitalism, renal abnormalities, retinal dystrophy, and several less frequently observed features. Eleven genes mutated in BBS patients have been identified, and more are expected to exist, since about 20–30% of all families cannot be explained by the known loci. To investigate the etiopathogenesis of BBS, we created a mouse null for one of the murine homo-

logues, *Bbs4*, to assess the contribution of one gene to the pleiotropic murine Bbs phenotype. *Bbs4* null mice, although initially runted compared to their littermates, ultimately become obese in a gender-dependent manner, females earlier and with more severity than males. Blood chemistry tests indicated abnormal lipid profiles, signs of liver dysfunction, and elevated insulin and leptin levels reminiscent of metabolic syndrome. As in patients with BBS, we found age-dependent retinal dystrophy. Behavioral assessment revealed that mutant mice displayed more anxiety-related responses and reduced social dominance. We noted the rare occurrence of birth defects, including neural tube defects and hydrometrocolpos, in the null mice. Evaluations of these null mice have uncovered phenotypic features with age-dependent penetrance and variable expressivity, partially recapitulating the human BBS phenotype.

Electronic Supplementary Material Supplementary material is available to authorised users in the online version of this article at <http://dx.doi.org/10.1007/s00439-006-0197-y>.

E. R. Eichers · R. Paylor · R. A. Lewis · W. Bi · X. Lin ·
T. P. Meehan · D. W. Stockton · M. J. Justice ·
J. R. Lupski (✉)
Department of Molecular and Human Genetics,
Baylor College of Medicine,
One Baylor Plaza Room 604B,
Houston, TX 77030, USA
e-mail: jlupski@bcm.edu

M. M. Abd-El-Barr · R. Paylor · S. M. Wu
Department of Neuroscience,
Baylor College of Medicine,
Houston, TX 77030, USA

M. M. Abd-El-Barr · R. A. Lewis · D. W. Stockton ·
S. M. Wu
Department of Ophthalmology,
Baylor College of Medicine,
Houston, TX 77030, USA

R. A. Lewis · J. R. Lupski
Department of Pediatrics, Baylor College of Medicine,
Houston, TX 77030, USA

R. A. Lewis · D. W. Stockton
Department of Medicine, Baylor College of Medicine,
Houston, TX 77030, USA

E. Lindsay
Department of Pediatrics (Cardiology),
Baylor College of Medicine,
Houston, TX 77030, USA

D. W. Stockton · J. R. Lupski
Texas Children's Hospital, Houston, TX 77030, USA

P. L. Beales
Molecular Medicine Unit, Institute of Child Health,
University College London, London, WC1N 1EH, UK

N. Katsanis
McKusick-Nathans Institute of Genetic Medicine,
Johns Hopkins University, Baltimore, MD 21205, USA

N. Katsanis
Wilmer Eye Institute, Johns Hopkins University,
Baltimore, MD 21205, USA

Introduction

Bardet-Biedl syndrome (BBS) is a pleiotropic disorder, whose primary manifestations include progressive pigmentary retinopathy, learning difficulties, post-axial polydactyly, obesity, hypogenitalism, and renal abnormalities, although secondary features, such as speech pathology, diabetes mellitus, urogenital malformations, and congenital heart disease, also occur (Beales et al. 1999; Green et al. 1989). BBS is a model oligogenic disorder; mutations in eleven genes have been associated with the disorder thus far (Ansley et al. 2003; Badano et al. 2003a; Chiang et al. 2006; Chiang et al. 2004; Fan et al. 2004; Katsanis et al. 2001; Katsanis et al. 2000; Katsanis et al. 2002; Li et al. 2004; Mykytyn et al. 2001; Mykytyn et al. 2002; Nishimura et al. 2001; Nishimura et al. 2005; Slavotinek et al. 2000; Stoetzel et al. 2006). In most families, inheritance of the disorder seems to follow a traditional Mendelian autosomal recessive pattern; however, in some families, three mutations in two genes are required for disease manifestation (Badano et al. 2003b; Beales et al. 2003; Eichers et al. 2004; Katsanis et al. 2001; Katsanis et al. 2002) or the third mutant allele can apparently modify the severity of the trait (Badano et al. 2003b; Badano et al. 2006).

Animal models are useful to explore the basis of human disorders (Craigie 2001). To this end, several knockout mouse models of BBS have been engineered, including *Bbs4* (Kulaga et al. 2004; Mykytyn et al. 2004), *Bbs2* (Nishimura et al. 2004), *Bbs1* (Kulaga et al. 2004), and *Mkks/Bbs6* (Fath et al. 2005; Ross et al. 2005). These null mice exhibit some aspects of the BBS phenotype. In vitro studies with BBS4 showed that the protein localizes to the centriolar satellites of centrosomes and basal bodies of primary cilia (Kim et al. 2004). Combining this knowledge with observations of animal models led to the identification of anosmia in *Bbs4* null mice; subsequently this previously unrecognized trait has been found in human subjects with BBS (Kulaga et al. 2004). More recent studies of both mouse and zebrafish models have revealed a novel relationship between BBS proteins and the planar cell polarity (PCP) pathway (Ross et al. 2005).

Here we dissect the consequences of *Bbs4* loss of function in the mouse using a broad range of phenotypic analyses in a large cohort of animals. Previous published reports of *Bbs4* null mice have demonstrated that the mice exhibit skewed Mendelian ratios, obesity, photoreceptor degeneration, anosmia, neural tube defects, and some behavioral anomalies (Kulaga et al. 2004; Mykytyn et al. 2004; Nishimura et al. 2004; Ross et al. 2005). We describe here novel phenotypes of the *Bbs4* null mice, including evidence for a

gender-specific difference in obesity as well as quantitative data regarding the body composition of the mice, characteristics reminiscent of metabolic syndrome and mild liver dysfunction, definition of the retinal phenotype as a cone-rod dystrophy, and elevated anxiety-related responses.

During the expansion of the *Bbs4* mouse colony, we found fewer than expected null pups relative to heterozygous and wild-type mice and attributed this finding to decreased perinatal survival rather than embryonic lethality. We found that the null *Bbs4* mice, although initially runted compared to their littermates, later become obese in a progressive and gender-dependent manner. The obesity, combined with abnormal serum lipid profiles and elevated plasma insulin and leptin levels, suggest that the null animals manifest phenotypes consistent with metabolic syndrome. Blood chemistry tests also indicated the null mice have abnormal liver enzymes and blood urea nitrogen (BUN) levels, among others. Age-dependent pigmentary retinal dystrophy was detected in the null mice by ophthalmoscopy and confirmed by histologic and electrophysiologic studies, the latter detecting changes earlier than the other methods. A battery of behavioral tests demonstrated that the null mice display increased anxiety-related responses and less social dominance than their littermates. The rare occurrence of major birth defects including neural tube defects, which stimulated further evaluation of the PCP pathway (Ross et al. 2005), and hydrometrocolpos was noted in the *Bbs4* null mice. Hydrometrocolpos, or fluid accumulation in the uterus, is reminiscent of human patients with the McKusick–Kaufman syndrome (MKKS), the majority of whom harbor mutations in *MKKS/BBS6*. Polydactyly was never observed.

Absence of the *Bbs4* gene alone is insufficient to recapitulate the full spectrum of the BBS phenotype, but many features of the human phenotype are found in the animal model; although none are fully penetrant. These findings are consistent with the variability seen both within and between BBS patients and families, the complex inheritance patterns in this syndrome, including modifier genes (Badano et al. 2003b; Badano et al. 2006), and the possible influence of genetic background.

Materials and methods

Generation of the *Bbs4* mouse model

To make the mouse model, embryonic stem cells (of 129/SvEv origin) carrying a gene trap insertional

mutation in the first intron of *Bbs4* were obtained from Lexicon Genetics Incorporated (Kulaga et al. 2004). Blastocyst injections and transfer to C57BL/6J-*Tyr^{c-2l}*/J pseudopregnant mothers were completed at the Darwin Transgenic Mouse Core Facility, Baylor College of Medicine. Heterozygous mice of the N2 generation were intercrossed to yield wild-type, heterozygous, and null mice for these studies. Both reverse transcriptase PCR and real-time PCR were performed on total RNA isolated from mouse liver with *Bbs4*-specific primers to confirm the absence of *Bbs4* transcript in the null animals (Supplementary Fig. 1a, b). Mice were genotyped by Southern blotting or PCR analysis of mouse genomic DNA isolated from tail clips (Kulaga et al. 2004).

Viability

Mating cages were monitored daily for birth of pups. Pups that did not survive were removed from the cages for DNA isolation and genotyping. For embryo analysis, we arranged additional timed matings and females were checked daily for vaginal plugs. At 18.5 days of gestation, pregnant females were euthanized with an overdose of 5% avertin solution (0.032 ml/g body weight). Embryos were dissected from the uterus and weighed; subsequently the embryo tails were clipped for DNA extraction and genotyping. Following screening for gross morphological defects, we removed the chest walls of embryos, and fixed the whole embryos in 10% neutral buffered formalin. After fixation, embryos were transferred to 70% ethanol and examined for gross heart defects.

Obesity

A minimum of ten mice of each gender and each genotype were weighed weekly, beginning at age 2 weeks. Weights were averaged by postnatal ages and error bars represent the standard error of the mean (SEM). An individual mouse was determined to be obese if its weight was greater than the mean weight+2 SDs of its age- and gender-matched wild-type littermates.

Adult mice at least seven months of age were analyzed with a Bruker minispec NMR Live Mice Analyzer (Bruker Optics Inc., Billerica, MA, USA) to determine fat mass, lean mass, and fluid mass ($N \geq 18$). The mean of each mass was calculated, and the error bars indicate the SEM. Additionally, the percentages of fat mass, lean mass, and fluid mass of the total body mass (at the time of the experiment) of the mice were calculated. Error bars represent the SEM.

Abdominal fat pads and whole livers were dissected at the time of necropsy and weighed. Livers were

fixed in 10% neutral buffered formalin for 24 h then transferred to 70% ethanol. The tissue was dehydrated with a series of ethanol washes and embedded in paraffin for sectioning; 4 μ m sections were prepared. Hematoxylin and eosin stained slides were photographed under light microscopy at a final magnification of 200 \times .

Serum and plasma analyses

Blood samples were collected via cardiac puncture from fasted mice 4–6 months of age immediately following CO₂-induced unconsciousness ($N \geq 8$ of each gender and genotype). Serum was separated from the whole blood with Serum-Gel clotting activator micro tubes (Sarstedt, Newton, NC, USA). Serum samples were analyzed at the Comparative Pathology Laboratory, Baylor College of Medicine with the COBAS INTEGRA[®] 400 *plus* analyzer (Roche, Alameda, CA, USA). Plasma was prepared from whole blood by adding EDTA to a final concentration of 0.5% and centrifuging at 1,000g for 5 min at 4°C. Plasma insulin levels from ten null and eight wild-type mice were measured with a Rat Insulin ELISA Kit (Crystal Chem Inc., IL, USA). Plasma leptin levels from 11 null and nine wild-type mice were measured with the Mouse Leptin Quantikine ELISA Kit (R&D Systems, MN, USA). Two-way ANOVA tests were performed to establish significance and test for interaction between genders and genotypes.

Retinal analysis

A single examiner (RAL) performed all retinal examinations in a masked fashion with a conventional indirect ophthalmoscope and a 78 diopter hand-held condensing lens following dilation of each eye with one drop of 1% tropicamide (Falcon Pharmaceuticals, Ltd., Fort Worth, TX, USA). For this experiment, 26 null, 16 heterozygous, and 25 wild-type mice were studied. Fundus photographs were obtained with a Genesis Small Lab Animal Fundus Camera (Kowa, Torrance, CA, USA).

For histological analysis, mouse eyes were enucleated and fixed for 24 h in Fekete's fixative. The eyes were dehydrated in sequential ethanol washes and embedded in paraffin; 4 μ m sections were prepared. Slides were stained with hematoxylin and eosin and photographed under light microscopy at a final magnification of 200 \times .

Electroretinography was performed on overnight dark-adapted mice at the ages of four ($N=10$ null), eight ($N=4$ null), and 14 weeks ($N=8$ null) as described

(Pennesi et al. 2003). Data from wild-type mice of the three ages were pooled ($N=7$). To analyze rod function, a saturating light estimated to produce approximately $2.92 \log \text{scot cd s m}^2$, or an estimated 800,000 photoisomerizations/rod, for normal outer segment length was used to measure a_{\max} . To analyze the scotopic (dark-adapted) b -wave, which is an extracellular field potential thought to be primarily from ON-rod bipolar cells (Hood and Birch 1996), increasing stimulus intensities and b -wave amplitude was fit to a hyperbolic saturation function (Naka-Rushton) (Bramblett et al. 2004). This model yields two parameters, $b_{\max, \text{scot}}$, the b -wave amplitude, and $I_{0.5}$, the intensity of light at which half of the photoreceptors are saturated. Cone-driven responses were recorded with the paired flash technique (Pepperberg et al. 1997). The first flash drove both the rods and cones temporarily into saturation. The second flash, delivered 2.5 s later, was sufficiently delayed to allow the cones, but not the rods, to recover.

Behavioral assessment

Behavioral testing of female and male two month old wild-type and null mice ($N \geq 10$ for each group) included locomotor activity in an open field, exploration of the light–dark box, acoustic startle response and prepulse inhibition of the acoustic startle response, and Pavlovian conditioned fear. These tests were performed and statistical analyses done as described (Walz et al. 2004). We also performed an assessment of balance with an accelerating rotarod that increased from 4–40 rpm over a 5 min trial period. Eight trials were performed per mouse. Additionally, we conducted a social dominance tube test in which one wild-type mouse and one null mouse were placed at opposite ends of a tube. The first mouse to back out of the tube was deemed to have lost the test, and the mouse remaining in the tube was given the win (Spencer et al. 2005). Each mouse was used only one time in this experiment and was paired with an opponent with whom it had not been housed. Statistical analysis for the tube test was performed with the chi-squared test as described (Spencer et al. 2005).

Results

Evidence for perinatal lethality of *Bbs4* null animals

During mouse colony expansion, the distribution of genotypes among offspring of N2 heterozygous mating pairs appeared to deviate from expected Mendelian ratios (25% wild-type : 50% heterozygous : 25% null).

After genotyping 504 pups from 10 different mating pairs, we determined that 129 (26%) were wild-type, 288 (57%) were heterozygous, and 87 (17%) were homozygous null ($P < 0.001$). We also noted that, of those pups born, not all survived the neonatal period. We found that among the 50 decedent pups, seven were wild-type, 19 were heterozygous, and 24 were null. The neonatal survival rate of the null pups was statistically less than that of their unaffected littermates ($P < 0.001$) when we compared our ratios to those expected if each genotype had an equal chance of survival. No gross external abnormalities were observed in the dead pups. To establish if the skewed Mendelian ratios could be attributed to embryonic lethality, we collected E18.5 embryos from heterozygous mating pairs. Of the 111 developed embryos, 29 were wild-type (26%), 52 were heterozygous (47%) and 30 (27%) were null. These ratios are not significantly different from the expected Mendelian ratios ($P = 0.79$). During embryo collection, we also observed ten absorbed embryos. The lack of skewed ratios at E18.5, and a disproportionate number of null pups dead perinatally, suggests that perinatal death is the likely cause of the deviant Mendelian ratios.

We examined null embryos at E18.5 for gross heart defects to discern if such abnormalities could be contributing to the perinatal demise of the null pups. None of the 12 null embryos which we examined had any obvious evidence of gross heart abnormalities, potentially lethal postnatally. During their collection, we weighed the embryos to determine if the null pups were runt compared to their littermates. We found no significant difference in the weight of E18.5 embryos between genotypes ($P = 0.59$, data not shown), even though the null pups were statistically smaller at two weeks postnatally.

Earlier onset and more severe obesity in *Bbs4* females

Obesity, typically by the end of the first year of life, is a primary diagnostic feature of BBS. To evaluate the *Bbs4* mice for this phenotype, mice were weighed weekly, beginning at 2 weeks postnatally ($N \geq 10$ for each group at each time). At 2 weeks of age, all null mice were runt compared to their littermates (Fig. 1a). Female null mice remained significantly underweight compared to their heterozygous and wild-type littermates until 10 weeks of age ($P < 0.05$; Fig. 1c), whereas male null mice were smaller until 12 weeks old ($P < 0.05$; Fig. 1d). With time, both male and female populations of null mice become obese (Fig. 1b); however, not every null mouse became obese. Female null mice were significantly overweight by week 13 ($P < 0.05$;

Fig. 1c), whereas male mice were not overweight statistically until week 24 ($P < 0.05$; Fig. 1d). Up to 92% of the female and 40% of the male null mice were determined to be obese (as defined by > 2 SDs above the average weight of gender- and age-matched wild-type mice). Among females, the difference in weights between null mice and their littermates was greater than in the male population. Thus, the obesity is more severe and has earlier onset in females than males.

To characterize the increased body weight of the mice, we applied nuclear magnetic resonance (NMR) to quantify lean, fat, and fluid mass in adult null mice and their littermates ($N \geq 18$ for each genotype and gender). Among both male and female mice, the null animals have significantly greater fat and fluid masses but not lean mass ($P < 0.001$; Fig. 1e, h). Additionally, computing the portion of each measurement of total body mass, the null mice have significantly greater fat and fluid mass fractions, and a significantly less lean mass fraction ($P < 0.001$; Fig. 1f, i). The null mice in this experiment were obese compared to their heterozygous and wild-type counterparts ($P < 0.001$ for females and $P = 0.001$ for males; Fig. 1g, j).

At necropsy, organs and abdominal fat were dissected out from the mice and weighed. The null animals had a significantly larger quantity of abdominal fat ($P < 0.01$ for both male and female; $N \geq 10$ for each group; Fig. 2a), consistent with the NMR analysis in suggesting that the increase in body weight is attributable to fat accumulation. Additionally, males had a significantly larger liver ($P < 0.01$; $N \geq 10$ for each group; Fig. 2b), presumably due to the increase in fat deposits noted during histological examination (Fig. 2c, d).

Metabolic disturbances and evidence for mild liver dysfunction

We tested serum or plasma to identify major abnormalities in kidney or liver function and to monitor other metabolic anomalies. Significant results ($P \leq 0.05$) of these analyses are summarized as Table 1. Except where noted, serum was the reagent examined and gender did not influence the results. Analyses of the lipid panel results demonstrated that the null mice had significantly elevated levels of total cholesterol, high-density lipoprotein (HDL)-cholesterol, low-density lipoprotein (LDL)-cholesterol, very low-density lipoprotein (VLDL)-cholesterol, and triglycerides. Additionally, the null mice had a significant increase in the ratio of total cholesterol to HDL-cholesterol. A positive correlation was seen between body weight and HDL-cholesterol levels in the null animals (data not shown). Plasma insulin and leptin levels were also ele-

vated in the null mice. The increase in cholesterol, triglyceride, insulin, and leptin levels, combined with the obesity, is reminiscent of metabolic syndrome. Elevated blood glucose levels were also found in the mice.

Several results suggest abnormal liver function in the null mice compared to unaffected littermates. Null mice had elevated amounts of alanine aminotransferase (ALT) and aspartate aminotransferase (AST), but only females had increased alkaline phosphatase (ALP) levels. The null mice also manifested significantly higher levels of lactate dehydrogenase (LDH). In the male *Bbs4* null mice, we found elevated total and insoluble bilirubin, indicating that the liver may not be solubilizing indirect bilirubin to direct bilirubin properly. These abnormal results may be associated with fat deposit accumulation in the livers of the obese animals (Fig. 2c, d).

The null mice have elevated blood magnesium, sodium, and BUN levels. A decreased ratio of albumin to globulin and a significant increase in globulin levels were also detected in the null animals. The null mice have elevated levels of creatine kinase (CK). The explanation for these differential responses is not apparent.

No significant differences between genotypes were observed in levels of albumin, total protein, direct bilirubin, creatinine, osmolarity, potassium, calcium, or phosphorus (data not shown).

Age-dependent retinopathy with cone dysfunction more prominent than rod dysfunction

To analyze the retinal phenotype, we took a three-tier approach. First, a single observer (RAL) performed indirect ophthalmoscopy in a masked fashion at various stages of postnatal development. The retinal appearance was scored on a progressive scale of 1–4, with “normal” being no detectable abnormalities. A score of “1” represented a granular fundus appearance, “2” denoted addition of vascular attenuation, “3” optic nerve atrophy, and “4” gross pigmentary retinopathy. Mice of each genotype were followed for a period of 11 months (Fig. 3a–c). By the end of the observation period, the wild-type and heterozygous mice maintained a “normal” score, whereas 20% of the null mice were considered “normal.” Only null mice progressed to a score of “3” or “4” during the course of the observations, with 80% of the null mice reaching these states by 11 months of age. To document the fundus phenotype, fundus photographs show three female littermates at 10 months of age (Fig. 3d–f); only the null mouse exhibits an abnormal retinal phenotype. To document the progression of the retinopathy, we took

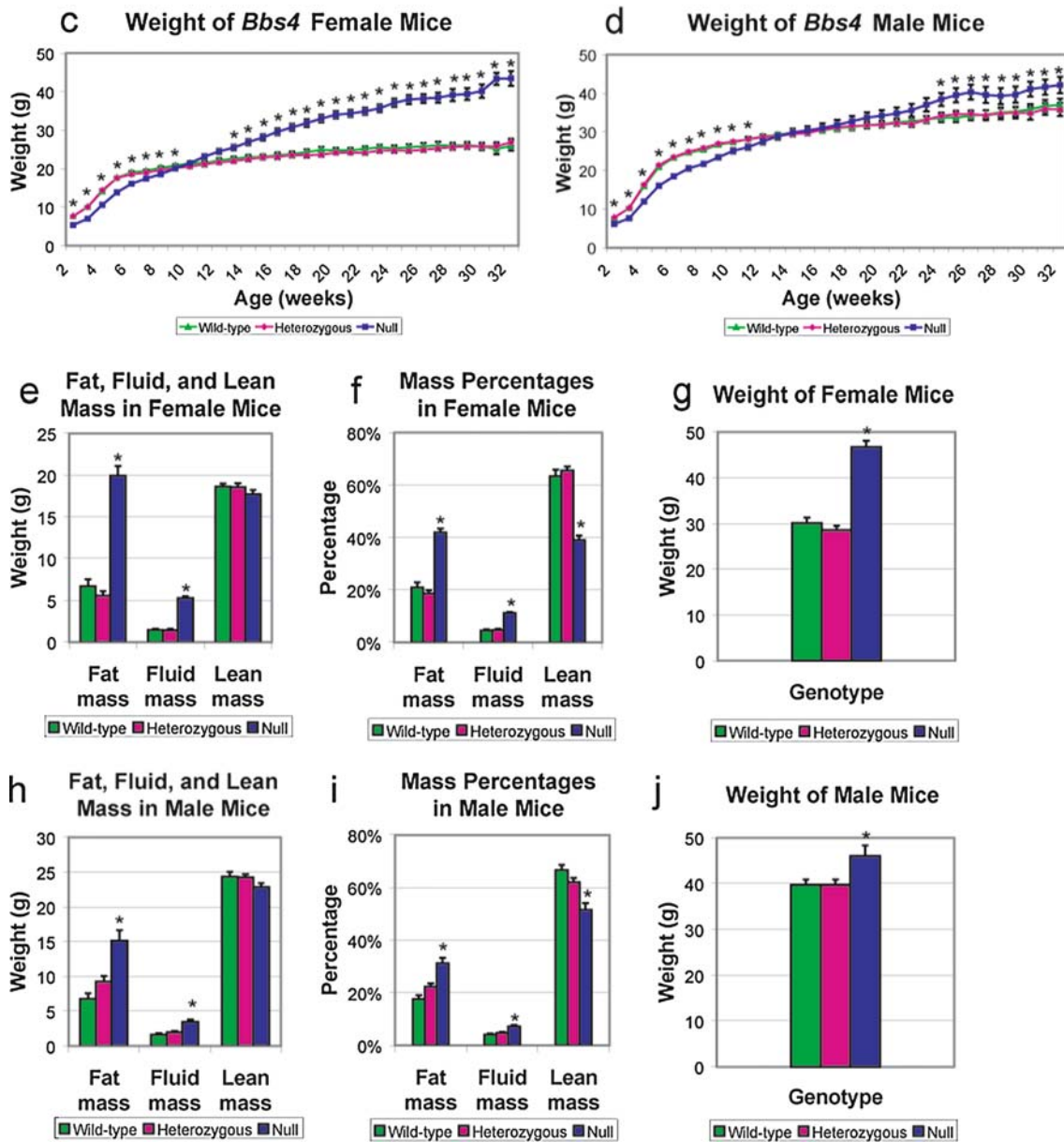
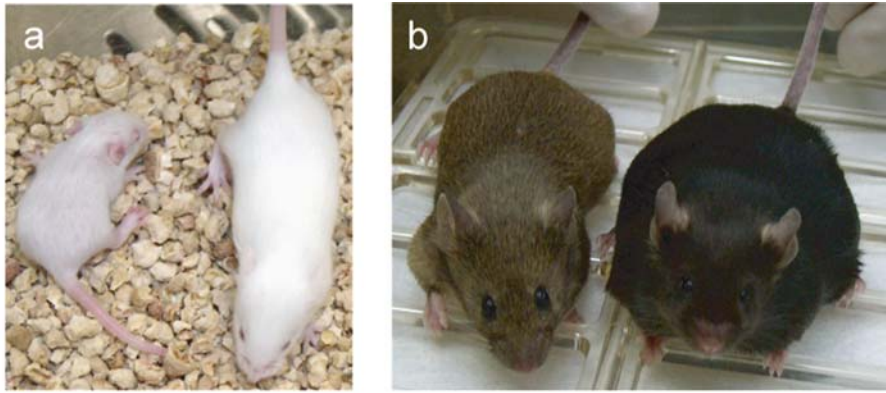




Fig. 1 Weight and body composition analysis of *Bbs4* mice. **a** Null mice are runt when they are young; the null mouse is on the left and a wild-type littermate is on the right. Over time, the null mice become obese; **b** shows two female littermates at 24 weeks; the wild-type mouse on the left weighs 28.7 g whereas the null mouse weighs 50.0 g. *Weight curves* of *Bbs4* mice over time for both females (**c**) and males (**d**), indicating the mice progress from significantly underweight to significantly overweight. Average fat, fluid, and lean masses of adult *Bbs4* female (**e**) and male (**h**) mice of each genotype ($N \geq 18$). For both genders, the fat

and fluid masses, but not lean mass, are significantly elevated in the null mice as compared to their counterparts. Averages of total body weight attributable to fat, fluid and lean masses are shown for females (**f**) and males (**i**). Null mice have significantly increased percentages of their body weight attributable to fat and fluid masses, and significantly less of a percentage due to lean mass. The average weight of the animals used for this experiment is shown for females in (**g**) and males in (**j**). Error bars represent SEM. Each significant data point is denoted with an asterisk

photographs at 4 months and again at 10 months of age; examples from one wild-type and two null mice are shown as Fig. 3g–l. The retinas appear normal at 4 months of age (Fig. 3g–i) but at 10 months the null mice have a distinct, abnormal fundus appearance including vessel attenuation, confluent pigment migration, large atrophic lacunae, and optic nerve pallor and atrophy (Fig. 3j–l).

Second, we examined the structure of the cells in the eye via histological analysis. As anticipated, retinal anom-

alies were detectable at an earlier age histologically than by ophthalmoscopic observation. At age two weeks, stained eye sections of wild-type and null mice did not differ (Supplementary Fig. 2). However, as the null mice aged, the photoreceptor layer became progressively thinner with a loss of nuclei and shortening of the inner and outer segments, until the photoreceptors appeared as a single, sparse layer of nuclei at 28 weeks (Supplementary Fig. 2). No thinning of the photoreceptor layer was detected in the aged-matched wild-type mice.

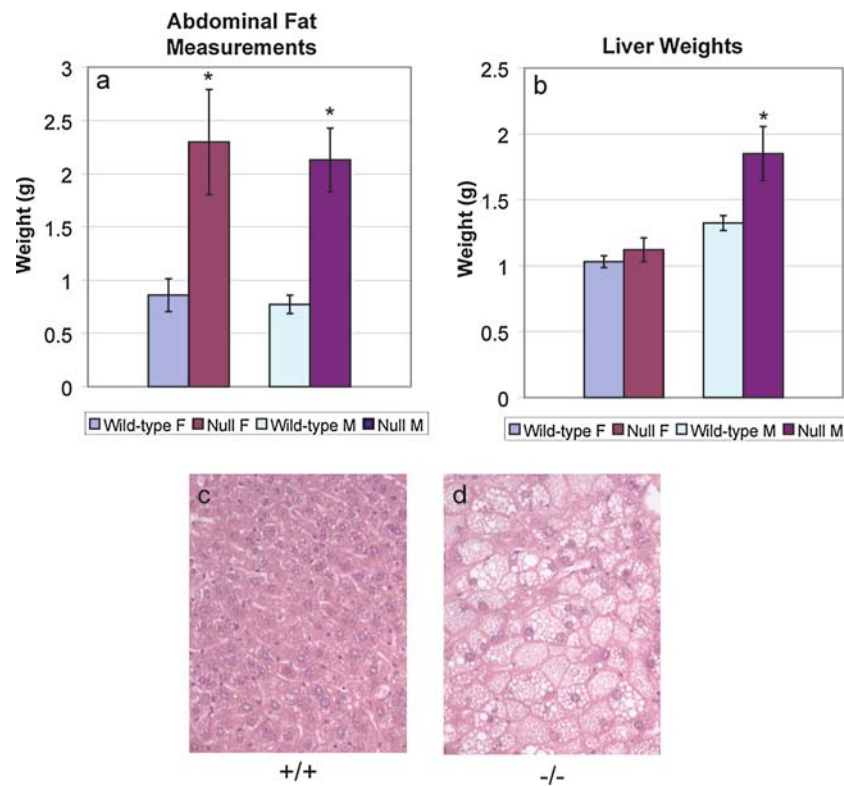


Fig. 2 Abdominal fat and liver necropsy data. **a** Weight of abdominal fat pads dissected out of wild-type and null males (*M*) and females (*F*) ($N \geq 10$ of each). The average abdominal fat from wild-type females was 0.86 g and of null females was 2.30 g ($P < 0.01$). For wild-type males the abdominal fat measurement was 0.77 g in the wild-type and 2.13 g in the null animals ($P < 0.001$). **b** Weight of total liver upon dissection from wild-type and null males and females

($N \geq 10$ of each). There was no significant difference in the liver weights of wild-type and null females (1.03 g and 1.12 g, respectively; $P = 0.35$). Null males had a significantly larger liver than their wild-type counterparts (1.85 g and 1.32 g, respectively; $P < 0.01$). Hematoxylin and eosin staining of liver sections from wild-type (**c**) and null (**d**) male mice demonstrate excess fat accumulation specifically in the obese null mouse

Table 1 Blood chemistry results

	+/+	-/-	P value
	Mean±SEM	Mean±SEM	
Total cholesterol (mg/dl)	84.19±4.61	131.18±8.89	0.000
HDL-cholesterol (mg/dl)	71.63±4.00	107.61±6.72	0.000
LDL-cholesterol (mg/dl)	12.22±0.60	16.40±1.47	0.005
VLDL-cholesterol (mg/dl)	21.59±1.39	31.35±2.79	0.001
cholesterol/HDL- cholesterol ratio	1.18±0.01	1.22±0.02	0.046
Triglycerides (mg/dl)	107.96±6.97	156.68±13.97	0.001
Glucose (mg/dl)	253.30±10.15	301.23±16.66	0.021
Insulin (ng/ml) ^a	1.16±0.16	2.41±0.40	0.015
Leptin (ng/ml) ^a	9.95±0.44	40.61±9.88	0.018
ALT (U/l)	23.19±1.82	50.00±9.05	0.004
ALP (U/l)	72.00±3.94	95.18±8.04	0.001 ^b
AST (U/l)	60.48±3.96	99.91±12.00	0.001
LDH (U/l)	185.78±13.85	404.91±59.15	0.000
Bilirubin total (mg/dl)	0.24±0.02	0.73±0.13	0.000 ^c
Indirect bilirubin (mg/dl)	0.26±0.03	0.74±0.15	0.001 ^c
Globulin (g/dl)	1.73±0.06	1.96±0.07	0.001
Albumin/globulin ratio	2.01±0.07	1.75±0.07	0.000
BUN (mg/dl)	21.26±0.87	26.11±1.27	0.002
Magnesium (mg/dl)	2.36±0.06	2.67±0.08	0.003
Sodium (mmol/l)	152.22±1.40	147.41±1.07	0.015
CK (U/l)	19.89±2.63	75±18.96	0.006

^a Plasma level^b Significant in females only^c Significant in males only

Our third and most sensitive method to document the progression of the retinal phenotype was electroretinography. Electroretinograms can provide information regarding photoreceptor function (*a*-wave) and the condition of the inner layers of the retina (*b*-wave). As early as four weeks postnatally, *Bbs4* null mice showed severe deterioration of both rod and cone responses. Photoreceptor function as evidenced by *a*-wave analysis showed that, at four weeks of age, *Bbs4* null animals had a significantly smaller a_{\max} compared to wild type (26% of wild-type value, $P<0.001$; Fig. 4a, b). By 8 weeks, a_{\max} had decreased to 22% ($P<0.001$; Fig. 4c) of wild-type and at 14 weeks the null a_{\max} was at 17% of the wild-type level ($P<0.001$; Fig. 4d; Table 2).

At 4 weeks, voltage responses of the scotopic *b*-wave indicated the null mice had a $b_{\max, \text{scot}}$ level of 58% of the wild-type ($P<0.01$; Fig. 4e, f). By 8 weeks, the null animals average a $b_{\max, \text{scot}}$ of 42% of the wild-type responses ($P<0.01$; Fig. 4g), and at 14 weeks this value was 22% of the wild-type response ($P<0.001$; Fig. 4h). Applying the Naka-Rushton fit to the scotopic *b*-wave data, a statistically insignificant increase in the half-saturating intensity $I_{0.5}$ was observed, potentially signifying a decrease in the sensitivity of the post-photoreceptor pathway.

Specifically focusing on the cone function, by 4 weeks of age the null mice had 12% of wild-type cone *b*-wave function ($P<0.001$; Fig. 4i, j) and by 8 weeks only 7% of the activity of the wild-type mice ($P<0.001$; Fig. 4k). At 14 weeks, the cone function remained almost completely deteriorated (7.7% of wild-type value, $P<0.001$; Fig. 4l).

Bbs4 mice are anxious and exhibit reduced social dominance

To determine if there are any behavioral phenotypes associated with the loss of *Bbs4* we carried out a battery of quantifiable behavioral tests (Crawley and Paylor 1997; McIlwain et al. 2001; Paylor et al. 2006). The open-field test evaluates exploratory activity and anxiety-related responses when mice are placed in an unfamiliar environment. We measured various parameters in this procedure, including total distance traveled, movement time, movement speed, rearing activity, and the center to total distance ratio. No significant differences between wild-type and null mice were observed for total distance traveled ($P=0.26$; Fig. 5a), movement time ($P=0.26$), and movement speed ($P=0.08$) (data not shown). However, the null mice have significantly less rearing activity ($P=0.03$; Fig. 5b) and have a smaller center to total distance ratio ($P=0.01$; Fig. 5c). The latter finding, demonstrating the null mice are avoiding the center of the open field, indicates the null mice have higher levels of anxiety-related responses than their littermates in the open field. Differences in rearing behavior can be associated with differences in basal exploration, altered motor coordination, or anxiety-related responses. Based on the data from the open-field and other motor tests, we suggest that the rearing differences are most consistent with an increase in anxiety-related responses. Statistical analyses did not indicate differences between genders.

We also used a light–dark box test to assess anxiety-related responses. We measured latency to enter the dark side of the box, total time spent in the dark, and the number of transitions between the dark and light sides of the box. The latency time to enter the dark was the same between wild-type and null mice ($P=0.74$; Fig. 5d). However, the null mice made fewer transitions between the dark and light sides of the box ($P<0.01$; Fig. 5e) and spent more total time in the dark ($P=0.02$; Fig. 5f). The increase in dark time and decrease in number of transitions indicates that the *Bbs4*-deficient mice have increased anxiety-related responses in the light–dark box test, which is consistent with the observations in the open-field test. Similar to the open-field test there was no interaction between genders and genotypes.

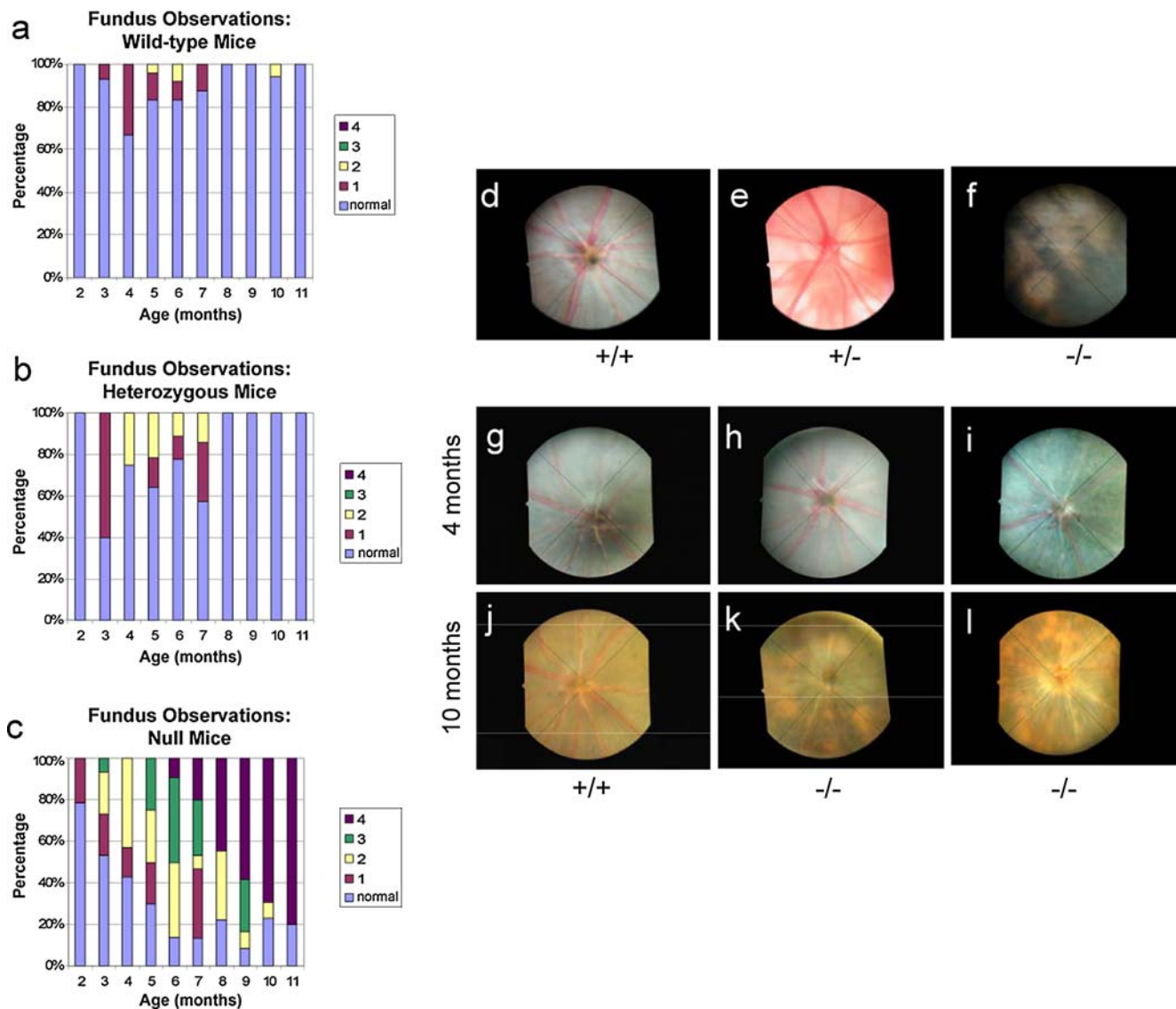


Fig. 3 Fundus observations and photography. *Bbs4* mice of all genotypes were subjected to direct fundus observation over a period of 11 months. For each time point, we calculated the percentage of mice with a normal fundus appearance, or with a score correlating to severity (on a scale of 1–4, with “4” being the most severe). Results for wild-type mice are seen in (a), heterozygous mice in (b), and null mice in (c). Fundus photographs documenting the pigmentary retinopathy specifically in the *Bbs4* null mice

are seen in (d–f); these photos are from 10-month-old female littermates. The progression of the retinal phenotype is documented in (g–l). The top panels (g–i) show fundus photographs taken when the mice were 4 months of age; g is from a wild-type mouse and h, j are from null mice. The bottom panel photographs (j–l) were acquired from the same mice at 10 months of age; j is wild-type and (k) and (l) are null. By 10 months, the gross pigmentary retinopathy was apparent in the null mice

As it has been previously reported in another *Bbs4* mouse model that the null animals exhibited a defect in social dominance (Nishimura et al. 2004), we wanted to evaluate our own mouse model for this phenotype. In 18 trials of the social dominance tube test, the wild-type mice won 15 trials and null mice won three. These results are statistically significant ($P < 0.005$; Fig. 5g) compared to a random probability, indicating that our null mice are also less socially aggressive than their wild-type littermates.

We observed no significant difference between wild-type and null mice in the rotarod (motor coordination

and skill learning), Pavlovian conditioned fear (learning and memory), acoustic startle response and prepulse inhibition of the acoustic startle response (assessing sensorimotor gating) experiments (Supplementary Fig. 3a–d).

Birth defects in null animals link *Bbs4* with PCP and MKKS

During our experiments, we observed two types of birth defects in our mice. In one female null mouse (of

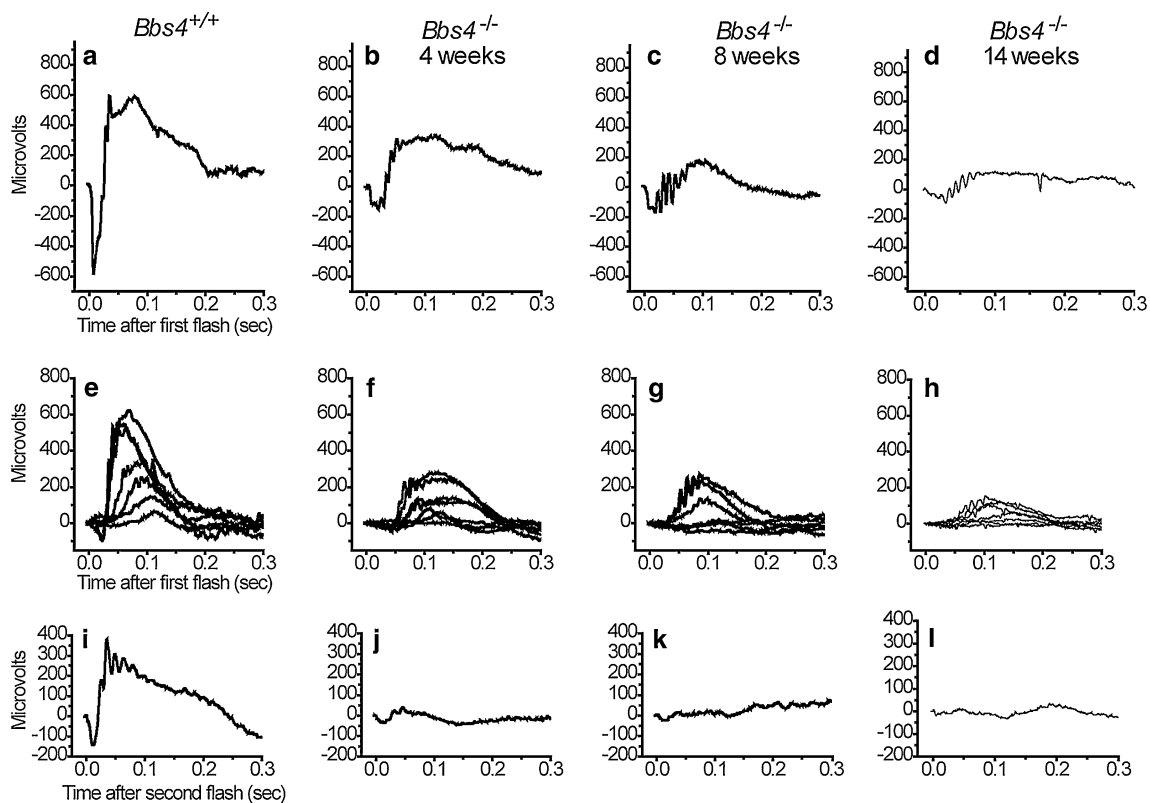


Fig. 4 Electretinography. Representative ERGs from wild-type and null *Bbs4* mice at four, eight and 14 weeks of age. ERG response to an intense flash (**a–d**). Measurement of the scotopic

b-wave (**e–h**). Each trace represents the average of at least five flashes. Cone isolated ERGs using the double flash method (**i–l**). Only the response to the second white flash is displayed

Table 2 ERG results

Group	a_{\max} (μV)	$b_{\max, \text{scot}}$ (μV)	$I_{0.5}$ (ϕ/rod)	Cone <i>b</i> -wave (μV)
<i>Bbs4</i> ^{+/+} ($n=7$; pooled ages)	578 \pm 54	626 \pm 72	4.39 \pm 1.5	311 \pm 30
<i>Bbs4</i> ^{-/-} ($n=10$; 4 weeks)	152 \pm 13 ^a	363 \pm 31 ^b	9.92 \pm 4	36 \pm 5 ^a
<i>Bbs4</i> ^{-/-} ($n=4$; 8 weeks)	129 \pm 33 ^a	263 \pm 52 ^b	4.44 \pm 1.4	23 \pm 9 ^a
<i>Bbs4</i> ^{-/-} ($n=8$; 14 weeks)	98 \pm 9 ^a	139 \pm 11 ^a	5.96 \pm 2.4	24 \pm 7 ^a

^a ($P < 0.001$)

^b ($P < 0.01$)

$N=22$), we observed hydrometrocolpos (Fig. 6a, b), a feature uncommon in BBS but characteristic of the similar allelic disorder, MKKS. Additionally, we found neural tube defects in 14% of null embryos ($N=50$), 1.4% of heterozygous embryos ($N=138$) and 0% of wild-type embryos ($N=65$) leading to midbrain exencephaly, one of several phenotypes shared between *Bbs* mice and mouse models with mutations in known PCP genes (Ross et al. 2005). The Mouse Genome Informatics database at The Jackson Laboratory (<http://www.informatics.jax.org>) indicates that neither of these phenotypes has been reported in the inbred 129/Sv or C57BL/6 strains.

Discussion

Animal models lacking expression of genes implicated in human disorders enables evaluation of the contribution of one gene to a particular complex phenotype as well as to deduce and analyze mechanisms of pathogenesis. For pleiotropic, oligogenic disorders such as BBS, the influence of each gene on specific aspects of the complex phenotype can be explored. For example, the *Bbs4*, *Bbs6*, and *Bbs2* mice share phenotypic features common to human BBS, such as obesity and retinal dystrophy; however, each gene causes the individual features to express uniquely. In this study,

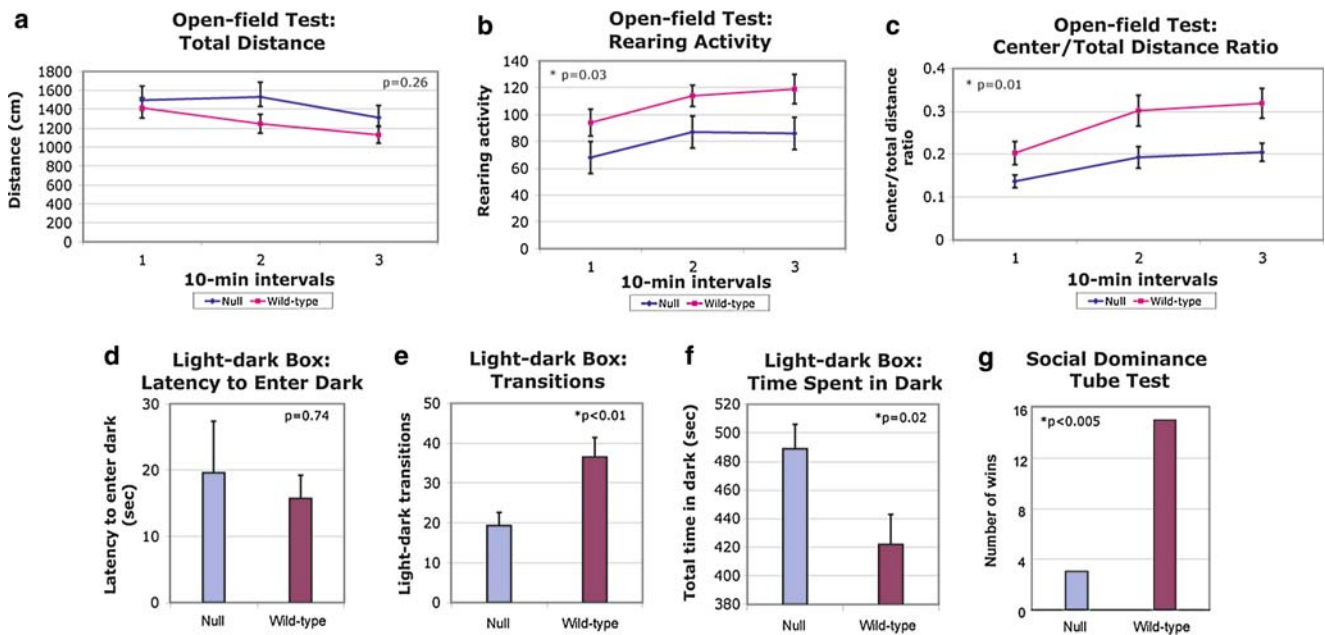


Fig. 5 Behavioral testing indicates *Bbs4* null mice are more anxious and less socially dominant than their littermates. Results from the open-field test indicate that although the overall distance traveled does not vary between the wild-type and null mice (**a** $P=0.26$), the null mice have significantly less rearing activity than the wild-type mice (**b** $P=0.03$) and have a smaller center to total distance ratio (**c** $P=0.01$). In the light–dark box test there was

no significant difference in the latency to enter the dark between the genotypes of mice (**d** $P=0.74$), but the null mice transitioned between the light and dark fewer times (**e** $P<0.01$) and spent more total time in the dark (**f** $P=0.02$). In the social dominance tube test, the wild-type mice won significantly more trials than the null mice, indicating the null mice exhibit reduced social dominance (**g**: $P<0.005$)



Fig. 6 Female mouse with hydrometrocolpos. One female *Bbs4* null mouse was found to have hydrometrocolpos, accumulation of fluid in the uterus. **a** shows the mouse prior to dissection and **b** is a photograph after dissection and isolation of the uterus

analysis of the *Bbs4* phenotype uncovered age-dependent penetrance and variable expressivity of the phe-

notypic characteristics. Although the population of null mice may be characterized by a specific phenotypic attribute, not every null mouse may exhibit that feature (obesity, for example). Some features, such as hydrometrocolpos and neural tube defects, are infrequent and do not characterize the population. Interestingly, no *Bbs* mouse model exhibits polydactyly, a cardinal finding described in 69–95% of BBS patients (Beales et al. 1999). *Situs inversus* is found at an elevated frequency in BBS patients as compared to the general population, but still identified only rarely in individuals diagnosed with BBS. No instances of this condition have been observed in *Bbs* mice. Because our mice are a mix of two strains (129/SvEv and

Table 3 Penetrance levels of mouse *Bbs4* phenotypes

Phenotype	Penetrance (%)	<i>N</i> of null mice
Obesity	92% Female, 40% Male	$N \geq 10$ for each gender and time point
Retinal dystrophy	80	26
Polydactyly	0	20
Birth defects		
Hydrometrocolpos	4.5	22
Neural tube defects	14	50
<i>Situs inversus</i>	0	20

C57BL/6J-*Tyr^{c-2j}/J*), it is possible that some of the variability seen can be attributed to the mixed background. However, given the large number of mice studied in direct comparison to littermate controls, and given that some of the phenotypes observed and studied have never been reported in either inbred background strains, the contribution of genetic background was controlled to the extent possible. Table 3 provides a summary of the penetrance levels of phenotypes observed in our *Bbs4* mouse model.

We observed that null mice were not different in weight compared to their littermates at E18.5, but that after birth a significant portion of the null mice died and those that survived were noticeably and significantly smaller than their littermates. Direct observations did not indicate gross heart defects as a cause of perinatal lethality in the null animals. Because null mice have been determined to have anosmia, the failure to thrive is potentially a consequence of the inability of the pups to respond to olfactory cues from their mother, especially in litters from heterozygous mating pairs where competition is more intense for the null pups, as only 25% of the pups are expected to be of this genotype (Cooper and Cowley 1976; Hongo et al. 2000; Teicher et al. 1978). The null pups likely have more difficulty nipple-searching and suckling, as daily weight gain is a reliable indicator of successful suckling (Coppola et al. 1994). Consistent with this hypothesis, in the offspring of null \times heterozygous matings, the ratio of heterozygous to null offspring does not deviate from the expected Mendelian ratio of 50% heterozygous to 50% null ($N=46$, $P=0.77$). The increased survival of null pups in these litters may be attributable to less competition from non-null littermates; however, the presence of the heterozygous littermates is important in stimulating lactation in the mother (Cooper and Cowley 1976). We have also observed that in two litters born to a null \times null mating pair, no pups survived past two days of age. The reason these pups did not survive is probably a consequence of anosmia-related reduced suckling, which in turn leads to a decrease or even termination of maternal lactation (Cooper and Cowley 1976).

In the mouse models for BBS, obesity is attributable to a substantial increase in fat mass. A pilot experiment suggests obesity in some null mice may result from increased food consumption. The obesity is more severe and is observed earlier in female null mice as compared to males which suggests the possibility of a gender-dependent genetic modifier of this phenotype. The livers of the null mice are also enlarged, most likely due to the increase in fat deposits apparent upon histological examination of the liver (Fig. 2c, d).

Accordingly the serum profiles (liver function tests) are consistent with a fatty liver picture but to what extent this progresses to chronic liver disease remains to be determined. In human patients, there have been several case reports of hepatic involvement in BBS but rather than fatty infiltration as in these mice, generally the histological picture showed portal fibrosis and, in one case, included narrow bands of fibrous tissue bridging portal tracts producing a micronodular non-obstructive cirrhosis but with minimal hepatic dysfunction (Pagon et al. 1982; Ross et al. 1956). Two other cases had dilatation of the intrahepatic ducts associated with the dilatation of the common bile duct (Caroli syndrome) (Meeker and Nighbert 1971; Tsuchiya et al. 1977). Five other cases with hepatic pathology accompanied by polydactyly, blindness, mental retardation, and renal dysfunction have been reported and in hindsight may constitute a diagnosis of BBS (Dekaban 1969; Delaney et al. 1978; Proesmans et al. 1975).

Although the BUN levels are abnormal in the mice, the creatinine levels were generally normal, an indication of functioning kidneys. However, in null mice of at least 6 months of age, we have observed cystic structural changes involving predominantly the tubules and occasionally the glomeruli (data not shown). These observations are not dissimilar to the human syndrome in which there is a great deal of intrafamilial variability in the development of renal abnormalities and it is not possible to predict the onset of organ dysfunction.

The obesity is also correlated with an increase in cholesterol, triglyceride, and insulin levels, features of the metabolic syndrome; however, additional information regarding hypertension and clotting ability in the mice is needed to complete such a diagnosis. Null mice exhibited elevated leptin levels, which have also been associated with the components of metabolic syndrome (Franks et al. 2005; Zimmet et al. 1999). In humans, elevated lipid levels indicate a higher risk for atherosclerosis; however, such a risk is difficult to establish, as mouse lipid profiles indicate most cholesterol is carried on HDL (in humans, most cholesterol is associated with LDL), and many strains are resistant to atherosclerosis (Jawień et al. 2004). Nevertheless, in humans with BBS hypertension, dyslipidemia, insulin resistance, obesity and even dysfibrinogenemia are common associations constituting true metabolic syndrome and as such *Bbs*-deficient rodents may provide useful model systems in which to investigate the metabolic syndrome (Iannello et al. 2002). More extensive investigation is needed to determine the particular role of *Bbs4* in lipid and cholesterol metabolism.

Retinopathy is the best characterized aspect of BBS. In our mice, we analyzed the onset of retinopathy via

observational, histological, and electrophysiological analysis. Each method suggests progression of this phenotype with age. Based on our fundus observations, this phenotype also is variable in its age of onset, with 20% of null animals yet to manifest a detectable phenotype by 11 months. Such variability is also apparent in patients and early age of onset is associated in some instances with the addition of a third mutant allele (Badano et al. 2003b). Age-dependent abnormal ERGs have been reported in patients (Héon et al. 2005; Jacobson et al. 1990; Lavy et al. 1995; Riise et al. 1996a; Riise et al. 1996b; Rizzo et al. 1986; Shawkat et al. 1996). However, the literature is not definitive as to whether the rods or cone are affected first (Jacobson et al. 1990; Riise et al. 1996a). We examined the course of the retinal phenotype with serial ERGs to segregate effects on rod and cone functions. The null mice have both rod and cone dysfunction; the cone dysfunction is earlier in onset and greater in severity. These data support the cone-rod dystrophy described in human patients (Berson et al. 1968; Rizzo et al. 1986). Additionally, the statistically insignificant increase in the half-saturating intensity $I_{0.5}$ may signify a decrease in the sensitivity of the post-photoreceptor pathway. However, the increase in $I_{0.5}$ may be a result of attenuation of the maximum signal transduction seen by the decrease in the $b_{\max, \text{scot}}$. More in-depth experimentation to understand the mechanism of this retinopathy is warranted, including studies of ciliary structure dysfunction.

Although limited information is available regarding the behavioral abnormalities in patients, anecdotal observations of disinhibited, indifferent behavior and measured heightened levels of anxiety have been published (Barnett et al. 2002; Beales et al. 1999; Green et al. 1989). Using objective and quantitative behavioral tests we obtained substantial evidence for an increase in anxiety-related responses in both the open-field and light–dark box test, and reduced social dominance in our *Bbs4* null mice. However, to explore correlations further, more extensive data must be collected from both patients and animal models. These animal models may offer opportunities to study the effects of anxiolytic therapies for later human investigations.

Although the retinal degeneration could contribute to some of the behavioral phenotypes in the *Bbs4* null mice, we suggest that the pattern of behavioral responses is different from other inbred strains of mice with *rd/rd* mutations (e.g. FVB/N). In this current study the null mice had similar levels of activity in the open-field, however FVB/NJ mice have significantly higher levels of activity in the open-field relative to

many other strains (Bouwknicht and Paylor 2002). *Bbs4* null mice also displayed decreased center to total distance ratio in the open-field, and more time in the dark and fewer light–dark transitions in the light–dark box test relative to wild-type littermates. In contrast, FVB/NJ mice spend less time in the dark and have more transitions compared to many inbred strains (Bouwknicht and Paylor 2002). Finally, FVB/NJ mice have significantly impaired contextual fear conditioning relative to other inbred strains, but fear conditioning is normal in the *Bbs4* null mice. Therefore, we propose that the *Bbs4* null behavioral abnormalities are not necessarily the result of retinal degeneration, although additional studies may be needed to test this hypothesis.

We reported previously that our *Bbs4* mouse strain is anosmic (Kulaga et al. 2004). There have been differing reports regarding the influence of anosmia on behavior. Male mice that had their olfactory bulbs removed, thus becoming anosmic, have been reported to be less aggressive than control mice (Liebenauer and Slotnick 1996). In contrast to the bulbectomized male mice, it has been demonstrated that male mice with anosmia peripherally induced by intranasal application of zinc sulfate continued to display aggressive behavior they had exhibited prior to treatment (Edwards et al. 1972). This difference in behavior between bulbectomized mice and those with peripherally induced anosmia may be due to the fact that central nervous system tissue damage has been associated with postsurgical anosmia in bulbectomized mice (Edwards et al. 1972). Although the experimental setup and cause of anosmia in these two reports differs from our own, we cannot eliminate the possibility that the anosmia in our mice contributed to the lack of social dominance displayed in our own testing. Developmental delay is a primary feature of BBS patients, but we did not find any evidence of *Bbs4* involvement in learning and memory ability. This discrepancy suggests that other BBS genes or modifier genes contribute to this phenotype in patients; further testing of all *Bbs* animal models can help elucidate the molecular basis of the learning difficulties associated with BBS.

Hydrometrocolpos is a common manifestation in MKKS (McKusick et al. 1964), a disease phenotypically similar to BBS and also found to be associated with mutations in the *MKKS/BBS6* gene (Schaap et al. 1998; Stone et al. 2000). However, hydrometrocolpos has been reported infrequently in BBS patients, possibly because of definitional criteria and partially because of age-dependent phenotypic onset of pigmentary retinopathy later in the course of MKKS (David et al. 1999; Mehrotra et al. 1997; Stoler et al. 1995).

Neither hydrometrocolpos nor neural tube defects have been reported in *Bbs* mouse models previously. Additionally, neural tube defects are not a published feature of the human Bardet-Biedl phenotype.

This extensive characterization of the penetrance and variable expressivity of the *Bbs4* mouse model challenges for more extensive molecular analyses of the particular features observed. Additionally, knockout mice for the different *Bbs* genes offer options to study the oligogenic nature of BBS, including the ability of other *Bbs* alleles to potentially modify the penetrance and expression of several features of this disorder.

Acknowledgements We thank Isabel Lorenzo from the Darwin Transgenic Mouse Core Facility at Baylor College of Medicine for blastocyst injections and chimera production. At the Comparative Pathology Laboratory at Baylor College of Medicine we recognize Dr. Roger E. Price, Roxane Walden, and Vida Hortenstein for their aid with pathology, histology, and serum chemistry analysis, respectively. Additionally, we appreciate the statistical assistance of E. O'Brien Smith. ERE was supported in part by a National Science Foundation Graduate Teaching in Education Fellowship funded by grant number DGE-0086397. This work was also supported by the Baylor College of Medicine MRRD-DRC Neurobehavioral and Administrative Core Facilities, a March of Dimes grant to NK and JRL, and Public Health Service grant U01 HD 39372 to MJJ. RAL is a Senior Scientific Investigator of Research to Prevent Blindness, New York. SMW would like to acknowledge the following funding sources: NIH EY0446 and EY02520, Retina Research Foundation (Houston), and International Retina Research Foundation Inc. PLB is a Wellcome Trust Senior Research Fellow. This research was also funded by grants R01 HD42601, R01 DK072301, and R01 EY016859 to NK.

References

- Ansley SJ, Badano JL, Blacque OE, Hill J, Hoskins BE, Leitch CC, Kim JC, Ross AJ, Eichers ER, Teslovich TM, Mah AK, Johnsen RC, Cavender JC, Lewis RA, Leroux MR, Beales PL, Katsanis N (2003) Basal body dysfunction is a likely cause of pleiotropic Bardet-Biedl syndrome. *Nature* 425:628–633
- Badano JL, Ansley SJ, Leitch CC, Lewis RA, Lupski JR, Katsanis N (2003a) Identification of a novel Bardet-Biedl syndrome protein, BBS7, that shares structural features with BBS1 and BBS2. *Am J Hum Genet* 72:650–658
- Badano JL, Kim JC, Hoskins BE, Lewis RA, Ansley SJ, Cutler DJ, Castellani C, Beales PL, Leroux MR, Katsanis N (2003b) Heterozygous mutations in *BBS1*, *BBS2* and *BBS6* have a potential epistatic effect on Bardet-Biedl patients with two mutations at a second BBS locus. *Hum Mol Genet* 12:1651–1659
- Badano JL, Leitch CC, Ansley SJ, May-Simera H, Lawson S, Lewis RA, Beales PL, Dietz HC, Fisher S, Katsanis N (2006) Dissection of epistasis in oligogenic Bardet-Biedl syndrome. *Nature* 439:326–330
- Barnett S, Reilly S, Carr L, Ojo I, Beales PL, Charman T (2002) Behavioural phenotype of Bardet-Biedl syndrome. *J Med Genet* 39:e76
- Beales PL, Badano JL, Ross AJ, Ansley SJ, Hoskins BE, Kirsten B, Mein CA, Froguel P, Scambler PJ, Lewis RA, Lupski JR, Katsanis N (2003) Genetic interaction of *BBS1* mutations with alleles at other *BBS* loci can result in non-Mendelian Bardet-Biedl syndrome. *Am J Hum Genet* 72:1187–1199
- Beales PL, Elcioglu N, Woolf AS, Parker D, Flinter FA (1999) New criteria for improved diagnosis of Bardet-Biedl syndrome: results of a population survey. *J Med Genet* 36:437–446
- Berson EL, Gouras P, Gunkel RD (1968) Progressive cone-rod degeneration. *Arch Ophthalmol* 80:68–76
- Bouwknicht JA, Paylor R (2002) Behavioral and physiological mouse assays for anxiety: a survey in nine mouse strains. *Behav Brain Res* 136:489–501
- Bramblett DE, Pennesi ME, Wu SM, Tsai M-J (2004) The transcription factor *Bhlhb4* is required for rod bipolar cell maturation. *Neuron* 43:779–793
- Chiang AP, Beck JS, Yen H-J, Tayeh MK, Scheetz TE, Swiderski RE, Nishimura DY, Braun TA, Kim K-YA, Huang J, Elbedour K, Carmi R, Slusarski DC, Casavant TL, Stone EM, Sheffield VC (2006) Homozygosity mapping with SNP arrays identifies *TRIM32*, an E3 ubiquitin ligase, as a Bardet-Biedl syndrome gene (*BBS11*). *Proc Natl Acad Sci USA* 103:6287–6292
- Chiang AP, Nishimura D, Searby C, Elbedour K, Carmi R, Ferguson AL, Secrist J, Braun T, Casavant T, Stone EM, Sheffield VC (2004) Comparative genomic analysis identifies an ADP-ribosylation factor-like gene as the cause of Bardet-Biedl syndrome (BBS3). *Am J Hum Genet* 75:475–484
- Cooper AJ, Cowley JJ (1976) The effect of litter size on the growth, survival and behaviour of neonatal bulbectomised mice. *Biol Neonate* 29:56–65
- Coppola DM, Coltrane JA, Arsov I (1994) Retronasal or internal olfaction can mediate odor-guided behaviors in newborn mice. *Physiol Behav* 56:729–736
- Craigen WJ (2001) Mouse models of human genetic disorders. In: Scriver CR, Beaudet AL, Sly WS, Valle D (eds) *The metabolic and molecular bases of inherited disease*, vol 1. McGraw-Hill, New York, pp 379–415
- Crawley JN, Paylor R (1997) A proposed test battery and constellations of specific behavioral paradigms to investigate the behavioral phenotypes of transgenic and knockout mice. *Horm Behav* 31:197–211
- David A, Bitoun P, Lacombe D, Lambert J-C, Nivelon A, Vigneron J, Verloes A (1999) Hydrometrocolpos and polydactyly: a common neonatal presentation of Bardet-Biedl and McKusick-Kaufman syndromes. *J Med Genet* 36:599–603
- Dekaban AS (1969) Familial occurrence of congenital retinal blindness and developmental renal lesions. *J Genet Hum* 17:289–296
- Delaney V, Mullaney J, Bourke E (1978) Juvenile nephronophthisis, congenital hepatic fibrosis and retinal hypoplasia in twins. *Q J Med* XLVII:281–290
- Edwards DA, Thompson ML, Burge KG (1972) Olfactory bulb removal vs peripherally induced anosmia: differential effects on the aggressive behavior of male mice. *Behav Biol* 7:823–828
- Eichers ER, Lewis RA, Katsanis N, Lupski JR (2004) Triallelic inheritance: a bridge between Mendelian and multifactorial traits. *Ann Med* 36:262–272
- Fan Y, Esmail MA, Ansley SJ, Blacque OE, Boroevich K, Ross AJ, Moore SJ, Badano JL, May-Simera H, Compton DS, Green JS, Lewis RA, van Haelst MM, Parfrey PS, Baillie DL, Beales PL, Katsanis N, Davidson WS, Leroux MR (2004) Mutations in a member of the Ras superfamily of small GTP-binding proteins causes Bardet-Biedl syndrome. *Nat Genet* 36:989–993

- Fath MA, Mullins RF, Searby C, Nishimura DY, Wei J, Rahmoni K, Davis RE, Tayeh MK, Andrews M, Yang B, Sigmund CD, Stone EM, Sheffield VC (2005) Mks-null mice have a phenotype resembling Bardet-Biedl syndrome. *Hum Mol Genet* 14:1109–1118
- Franks PW, Brage S, Luan J, Ekelund U, Rahman M, Farooqi IS, Halsall I, O'Rahilly S, Wareham NJ (2005) Leptin predicts a worsening of the features of the metabolic syndrome independently of obesity. *Obes Res* 13:1476–1484
- Green JS, Parfrey PS, Harnett JD, Farid NR, Cramer BC, Johnson G, Heath O, McManamon PJ, O'Leary E, Pryse-Phillips W (1989) The cardinal manifestations of Bardet-Biedl syndrome, a form of Laurence-Moon-Biedl syndrome. *N Engl J Med* 321:1002–1009
- Héon E, Westall C, Carmi R, Elbedour K, Pantou C, MacKeen L, Stone EM, Sheffield VC (2005) Ocular phenotypes of three genetic variants of Bardet-Biedl syndrome. *Am J Med Genet* 132A:283–287
- Hongo T, Hakuba A, Shiota K, Naruse I (2000) Suckling dysfunction caused by defects in the olfactory system in genetic arhinencephaly mice. *Biol Neonate* 78:293–299
- Hood DC, Birch DG (1996) *b* wave of the scotopic (rod) electroretinogram as a measure of the activity of human on-bipolar cells. *J Opt Soc Am A* 13:623–633
- Iannello S, Bosco P, Cavaleri A, Camuto M, Milazzo P, Belfiore F (2002) A review of the literature of Bardet-Biedl disease and report of three cases associated with metabolic syndrome and diagnosed after the age of fifty. *Obes Rev* 3:123–135
- Jacobson SG, Borruat F-X, Apáthy PP (1990) Patterns of rod and cone dysfunction in Bardet-Biedl syndrome. *Am J Ophthalmol* 109:676–688
- Jawień J, Nastalek P, Korbut R (2004) Mouse models of experimental atherosclerosis. *J Physiol Pharmacol* 55:503–517
- Katsanis N, Ansley SJ, Badano JL, Eichers ER, Lewis RA, Hoskins BE, Scambler PJ, Davidson WS, Beales PL, Lupski JR (2001) Triallelic inheritance in Bardet-Biedl syndrome, a Mendelian recessive disorder. *Science* 293:2256–2259
- Katsanis N, Beales PL, Woods MO, Lewis RA, Green JS, Parfrey PS, Ansley SJ, Davidson WS, Lupski JR (2000) Mutations in *MKKS* cause obesity, retinal dystrophy and renal malformations associated with Bardet-Biedl syndrome. *Nat Genet* 26:67–70
- Katsanis N, Eichers ER, Ansley SJ, Lewis RA, Kayserili H, Hoskins BE, Scambler PJ, Beales PL, Lupski JR (2002) *BBS4* is a minor contributor to Bardet-Biedl syndrome and may also participate in triallelic inheritance. *Am J Hum Genet* 71:22–29
- Kim JC, Badano JL, Sibold S, Esmail MA, Hill J, Hoskins BE, Leitch CC, Venner K, Ansley SJ, Ross AJ, Leroux MR, Katsanis N, Beales PL (2004) The Bardet-Biedl protein *BBS4* targets cargo to the pericentriolar region and is required for microtubule anchoring and cell cycle progression. *Nat Genet* 36:462–470
- Kulaga HM, Leitch CC, Eichers ER, Badano JL, Lesemann A, Hoskins BE, Lupski JR, Beales PL, Reed RR, Katsanis N (2004) Loss of *BBS* proteins causes anosmia in humans and defects in olfactory cilia structure and function in the mouse. *Nat Genet* 36:994–998
- Lavy T, Harris CM, Shawkat F, Thompson D, Taylor D, Kriss A (1995) Electrophysiological and eye-movement abnormalities in children with the Bardet-Biedl syndrome. *J Pediatr Ophthalmol Strabismus* 32:364–367
- Li JB, Gerdes JM, Haycraft CJ, Fan Y, Teslovich TM, May-Simera H, Li H, Blacque OE, Li L, Leitch CC, Lewis RA, Green JS, Parfrey PS, Leroux MR, Davidson WS, Beales PL, Guay-Woodford LM, Yoder BK, Stormo GD, Katsanis N, Dutcher SK (2004) Comparative genomics identifies a flagellar and basal body proteome that includes the *BBS5* human disease gene. *Cell* 117:541–552
- Liebenauer LL, Slotnick BM (1996) Social organization and aggression in a group of olfactory bulbectomized male mice. *Physiol Behav* 60:403–409
- McIlwain KL, Merriweather MY, Yuva-Paylor LA, Paylor R (2001) The use of behavioral test batteries: effects of training history. *Physiol Behav* 73:705–717
- McKusick VA, Bauer RL, Koop CE, Scott RB (1964) Hydrometrocolpos as a simply inherited malformation. *JAMA* 189:813–816
- Meeker WR Jr, Nighbert EJ (1971) Association of cystic dilatation of intrahepatic and common bile ducts with Laurence-Moon-Biedl-Bardet syndrome. *Am J Surg* 122:822–824
- Mehrotra N, Taub S, Covert RF (1997) Hydrometrocolpos as a neonatal manifestation of the Bardet-Biedl syndrome. *Am J Med Genet* 69:220
- Mykytyn K, Braun T, Carmi R, Haider NB, Searby CC, Shastri M, Beck G, Wright AF, Iannaccone A, Elbedour K, Riise R, Baldi A, Raas-Rothschild A, Gorman SW, Duhl DM, Jacobson SG, Casavant T, Stone EM, Sheffield VC (2001) Identification of the gene that, when mutated, causes the human obesity syndrome *BBS4*. *Nat Genet* 28:188–191
- Mykytyn K, Mullins RF, Andrews M, Chiang AP, Swiderski RE, Yang B, Braun T, Casavant T, Stone EM, Sheffield VC (2004) Bardet-Biedl syndrome type 4 (*BBS4*)-null mice implicate *Bbs4* in flagella formation but not global cilia assembly. *Proc Natl Acad Sci USA* 101:8664–8669
- Mykytyn K, Nishimura DY, Searby CC, Shastri M, Yen H-j, Beck JS, Braun T, Streb LM, Cornier AS, Cox GF, Fulton AB, Carmi R, Lüleci G, Chandrasekharappa SC, Collins FS, Jacobson SG, Heckenlively JR, Weleber RG, Stone EM, Sheffield VC (2002) Identification of the gene (*BBS1*) most commonly involved in Bardet-Biedl syndrome, a complex human obesity syndrome. *Nat Genet* 31:435–438
- Nishimura DY, Fath M, Mullins RF, Searby C, Andrews M, Davis R, Andorf JL, Mykytyn K, Swiderski RE, Yang B, Carmi R, Stone EM, Sheffield VC (2004) *Bbs2*-null mice have neurosensory deficits, a defect in social dominance, and retinopathy associated with mislocalization of rhodopsin. *Proc Natl Acad Sci USA* 101:16588–16593
- Nishimura DY, Searby CC, Carmi R, Elbedour K, Van Maldergem L, Fulton AB, Lam BL, Powell BR, Swiderski RE, Bugge KE, Haider NB, Kwitek-Black AE, Ying L, Duhl DM, Gorman SW, Heon E, Iannaccone A, Bonneau D, Biesecker LG, Jacobson SG, Stone EM, Sheffield VC (2001) Positional cloning of a novel gene on chromosome 16q causing Bardet-Biedl syndrome (*BBS2*). *Hum Mol Genet* 10:865–874
- Nishimura DY, Swiderski RE, Searby CC, Berg EM, Ferguson AL, Hennekam R, Merin S, Weleber RG, Biesecker LG, Stone EM, Sheffield VC (2005) Comparative genomics and gene expression analysis identifies *BBS9*, a new Bardet-Biedl syndrome gene. *Am J Hum Genet* 77:1021–1033
- Pagon RA, Haas JE, Bunt AH, Rodaway KA (1982) Hepatic involvement in the Bardet-Biedl syndrome. *Am J Med Genet* 13:373–381
- Paylor R, Spencer CM, Yuva-Paylor LA, Pieke-Dahl S (2006) The use of behavioral test batteries, II: effect of test interval. *Physiol Behav* 87:95–102
- Pennesi ME, Howes KA, Baehr W, Wu SM (2003) Guanylate cyclase-activating protein (*GCAP*) 1 rescues cone recovery kinetics in *GCAP1/GCAP2* knockout mice. *Proc Natl Acad Sci USA* 100:6783–6788

- Pepperberg DR, Birch DG, Hood DC (1997) Photoresponses of human rods in vivo derived from paired-flash electroretinograms. *Vis Neurosci* 14:73–82
- Proesmans W, Van Damme B, Macken J (1975) Nephronophthisis and tapetoretinal degeneration associated with liver fibrosis. *Clin Nephrol* 3:160–164
- Riise R, Andréasson S, Tornqvist K (1996a) Full-field electroretinograms in individuals with the Laurence-Moon-Bardet-Biedl syndrome. *Acta Ophthalmol Scand* 74:618–620
- Riise R, Andréasson S, Wright AF, Tornqvist K (1996b) Ocular findings in the Laurence-Moon-Bardet-Biedl syndrome. *Acta Ophthalmol Scand* 74:612–617
- Rizzo JF III, Berson EL, Lessell S (1986) Retinal and neurologic findings in the Laurence-Moon-Bardet-Biedl phenotype. *Ophthalmology* 93:1452–1456
- Ross AJ, May-Simera H, Eichers ER, Kai M, Hill J, Jagger DJ, Leitch CC, Chapple JP, Munro PM, Fisher S, Tan PL, Phillips HM, Leroux MR, Henderson DJ, Murdoch JN, Copp AJ, Eliot M-M, Lupski JR, Kemp DT, Dollfus H, Tada M, Katsanis N, Forge A, Beales PL (2005) Disruption of Bardet-Biedl syndrome ciliary proteins perturbs planar cell polarity in vertebrates. *Nat Genet* 37:1135–1140
- Ross CF, Crome L, Mackenzie DY (1956) The Laurence-Moon-Biedl syndrome. *J Pathol Bacteriol* LXXII:161–172
- Schaap C, ten Tusscher MPM, Schrandt JJP, Kuijten RH, Schrandt-Stumpel CTRM (1998) Phenotypic overlap between McKusick–Kaufman and Bardet-Biedl syndromes: are they related? *Eur J Pediatr* 157:170–171
- Shawkat FS, Harris CM, Taylor DSI, Kriss A (1996) The role of ERG/VEP and eye movement recordings in children with ocular motor apraxia. *Eye* 10:53–60
- Slavotinek AM, Stone EM, Mykytyn K, Heckenlively JR, Green JS, Heon E, Musarella MA, Parfrey PS, Sheffield VC, Biesecker LG (2000) Mutations in *MKKS* cause Bardet-Biedl syndrome. *Nat Genet* 26:15–16
- Spencer CM, Alekseyenko O, Serysheva E, Yuva-Paylor LA, Paylor R (2005) Altered anxiety-related and social behaviors in the *Fmr1* knockout mouse model of fragile X syndrome. *Genes Brain Behav* 4:420–430
- Stoetzel C, Laurier V, Davis EE, Muller J, Rix S, Badano JL, Leitch CC, Salem N, Chouery E, Corbani S, Jalk N, Vicaire S, Sarda P, Hamel C, Lacombe D, Holder M, Odent S, Holder S, Brooks AS, Elcioglu NH, Da Silva E, Rossillion B, Sigaudy S, de Ravel TJJ, Lewis RA, Leheup B, Verloes A, Amati-Bonneau P, Mégarbané A, Poch O, Bonneau D, Beales PL, Mandel J-L, Katsanis N, Dollfus H (2006) *BBS10* encodes a vertebrate-specific chaperonin-like protein and is a major BBS locus. *Nat Genet* 38:521–524
- Stoler JM, Herrin JT, Holmes LB (1995) Genital abnormalities in females with Bardet-Biedl syndrome. *Am J Med Genet* 55:276–278
- Stone DL, Slavotinek A, Bouffard GG, Banerjee-Basu S, Baxevanis AD, Barr M, Biesecker LG (2000) Mutation of a gene encoding a putative chaperonin causes McKusick–Kaufman syndrome. *Nat Genet* 25:79–82
- Teicher MH, Flaum LE, Williams M, Eckhert SJ, Lumia AR (1978) Survival, growth and suckling behavior of neonatally bulbectomized rats. *Physiol Behav* 21:553–561
- Tsuchiya R, Nishimura R, Ito T (1977) Congenital cystic dilation of the bile duct associated with Laurence-Moon-Biedl-Bardet syndrome. *Arch Surg* 112:82–84
- Walz K, Spencer C, Kaasik K, Lee CC, Lupski JR, Paylor R (2004) Behavioral characterization of mouse models for Smith-Magenis syndrome and dup(17)(p11.2p11.2). *Hum Mol Genet* 13:367–378
- Zimmet P, Boyko EJ, Collier GR, de Courten M (1999) Etiology of the metabolic syndrome: potential role of insulin resistance, leptin resistance, and other players. *Ann N Y Acad Sci* 892:25–44